

Research Article

Adaptive Control with SSNN of UPFC System for the Compensation of Active and Reactive Power

¹A. Bouanane, ²A. Chaker and ¹M. Amara

¹Department of Electrical Engineering, Dr. Mouly Taher University of Saida, Algeria

²Department of Electrical Engineering, Enset Oran, Algeria

Abstract: The focus of this study is the effectiveness of the controller's Unified Power Flow Controller UPFC with the choice of a control strategy. This Unified Power Flow Controller (UPFC) is used to control the power flow in the transmission systems by controlling the impedance, voltage magnitude and phase angle. This controller offers advantages in terms of static and dynamic operation of the power system. It also brings in new challenges in power electronics and power system design. To evaluate the performance and robustness of the system, we proposed a hybrid control combining the concept of identification neural networks with conventional regulators and with the changes in characteristics of the transmission line in order to improve the stability of the electrical power network. With its unique capability to control simultaneously real and reactive power flows on a transmission line as well as to regulate voltage at the bus where it is connected, this device creates a tremendous quality impact on power system stability. The result which has been obtained from using MATLAB and SIMULINK software showed a good agreement with the simulation result.

Keywords: Adaptive control, ELMAN network, identification, robustness, stability, State Space Neural Network (SSNN), UPFC system

INTRODUCTION

As the power systems are becoming more complex, it requires careful design of the new devices for the operation of controlling the power flow in transmission system, which should be flexible enough to adapt to any momentary systems conditions. The operation of an ac power transmission line, are generally constrained by limitation of one or more network parameters and operating variables (Papic *et al.*, 1997).

FACTS is a technology introduced by Electrical Power Research Institute (EPRI) in the 80s (Narain and Laszlo, 1999). Its principle role is to Increase the transmission capacity of the ac lines and to control power flow over designated transmission lines. FACTS technologies involve conversion and switching of power electronics in the range of a few tens to few hundred megawatts (Gyugyi, 1992). New solid state self commutating devices such as MOSFETs, IGBTs, GTOs and also other suitable power electronic devices are used as controlled switches in FACTS devices (Narain and Laszlo, 2000). The universal and most flexible FACTS device is the Unified Power Flow Controller (UPFC). UPFC is the combination of three compensators' characteristic; i.e., impedance, voltage magnitude and phase angle, that are able to produce a more complete compensation.

Sen and Keri (2003) compared field results of the Inez UPFC project to an EMTP simulation. There are no details on the design of the controllers utilized, or the presence of any disturbances or uncertainties. Zhengyu *et al.* (2000) have discussed four principal control strategies for UPFC series element main control and their impacts on system stability. Ma (2003) demonstrated the feasibility of using a centralized optimal control scheme using an evolutionary programming algorithm. Sukumar (2006) has used a Radial Basis Function Neural Network (RBFNN) as a control scheme for the UPFC to improve the transient stability performance of a multimachine power system. Schoder *et al.* (2000) have proposed a Fuzzy damping controller. In last year's, the application of neural networks (NNs) for adaptive control has been a subject of extensive study (Xie *et al.*, 2006; Chau *et al.*, 2005; Chau, 2007; Lin *et al.*, 2006).

The method proposed in this study is novel. It combines two different approaches, namely intelligent techniques that seem to work but do not provide a formal proof and analytical techniques that provide proofs under some restricted conditions and for simple systems. These limitations have been a central driving force behind the creation of hybrid systems (Henriques and Dourado, 1999) where two or more techniques are combined in a manner that overcomes the limitations of individual techniques. So, the hybrid systems are

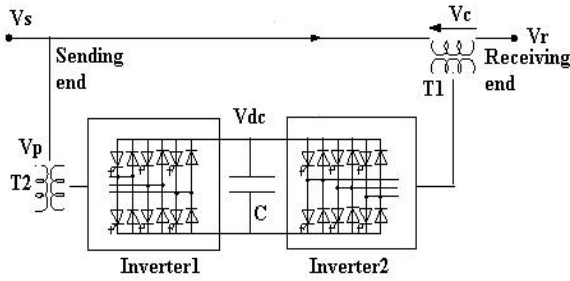


Fig. 1: Schematic diagram of three phases UPFC connected to a transmission line

important when considering the control of the unified power flow through a transmission line using a PWM-based UPFC, because, it is a complex application. The present study intends to be a contribution in this direction. It considers the application of adaptive Control, with neural networks in an electric power system.

UPFC CONSTRUCTION

The UPFC consists of two voltage source converters; series and shunt converter, which are connected to each other with a common dc link (Gyugyi, 1992; Edris *et al.*, 1996; Tuttas, 1999). Series converter or Static Synchronous Series Compensator (SSSC) is used to add controlled voltage magnitude and phase angle in series with the line, while shunt converter or Static synchronous Compensator (STATCOM) is used to provide reactive power to the ac system, beside that, it will provide the dc power required for both inverter. Each of the branches consists of a transformer and power electronic converter. These two voltage source converters shared a common dc capacitor (Xiang *et al.*, 2002).

The energy storing capacity of this dc capacitor is generally small. Therefore, active power drawn by the shunt converter should be equal to the active power generated by the series converter. The reactive power in the shunt or series converter can be chosen independently, giving greater flexibility to the power flow control.

The coupling transformer is used to connect the device to the system. Figure 1 shows the schematic diagram of the three phases UPFC connected to the transmission line. Control of power flow is achieved by adding the series voltage, V_s with certain amplitude. V_s and phase shift, ϕ to V_s . This will give a new line voltage V_c with different magnitude and phase shift. As the angle ϕ varies, the phase shift δ between V_c and V_r also varies.

Mathematical representation of UPFC: The simplified circuit of the control system and compensation of UPFC is shown in Fig. 2 modeling of

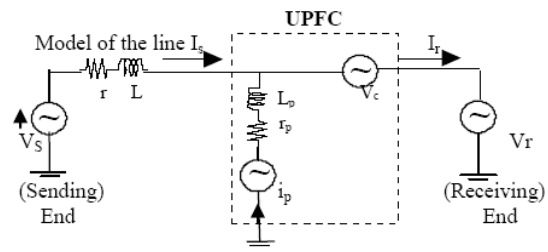


Fig. 2: Equivalent circuit of UPFC

this circuit is based on simplifying assumptions in the form of ideal voltage sources then the dynamic equations of the UPFC are divided into three systems of equations: the equations of the series branch, the equations of parallel branch and those of the DC circuit.

By applying Kirchhoff laws researchers will have the following equations for each branch.

The modeling of series branch: The mathematical model is given by the following Eq. (1):

$$\begin{aligned} \frac{di_{sa}}{dt} &= -\frac{r}{L} \cdot i_{sa} + \frac{1}{L} (v_{sa} - v_{ca} - v_{ra}) \\ \frac{di_{sb}}{dt} &= -\frac{r}{L} \cdot i_{sb} + \frac{1}{L} (v_{sb} - v_{cb} - v_{rb}) \\ \frac{di_{sc}}{dt} &= -\frac{r}{L} \cdot i_{sc} + \frac{1}{L} (v_{sc} - v_{cc} - v_{rc}) \end{aligned} \quad (1)$$

The transformation of Park aims to model this three-phase system (a, b, c) in two-phase (d, q) as follows:

$$\begin{bmatrix} x_d \\ x_q \\ x_o \end{bmatrix} = \frac{2}{3} \begin{bmatrix} \cos(\omega t) & -\sin(\omega t) & 1/2 \\ \cos(\omega t - 120^\circ) & -\sin(\omega t - 120^\circ) & 1/2 \\ \cos(\omega t + 120^\circ) & -\sin(\omega t + 120^\circ) & 1/2 \end{bmatrix}^T \begin{bmatrix} x_a \\ x_b \\ x_c \end{bmatrix} \quad (2)$$

where, x can be a voltage or current. In the case, the component x_o is not seen as the power system is assumed to be symmetric. After the transformation of Park, Eq. (1) is expressed in the dq reference by the equations:

$$\begin{aligned} \frac{di_{sd}}{dt} &= \omega \cdot i_{sq} - \frac{r}{L} \cdot i_{sd} + \frac{1}{L} (v_{sd} - v_{cd} - v_{rd}) \\ \frac{di_{sq}}{dt} &= -\omega \cdot i_{sd} - \frac{r}{L} \cdot i_{sq} + \frac{1}{L} (v_{sq} - v_{cq} - v_{rq}) \end{aligned} \quad (3)$$

The matrix form of the dq axis can be rewritten as follows:

$$\frac{d}{dt} \begin{bmatrix} i_{sd} \\ i_{sq} \end{bmatrix} = \begin{bmatrix} -r/l & +\omega \\ -\omega & -r/l \end{bmatrix} \begin{bmatrix} i_{sd} \\ i_{sq} \end{bmatrix} + \frac{1}{l} \begin{bmatrix} v_{sd} - v_{cd} - v_{rd} \\ v_{sq} - v_{cq} - v_{rq} \end{bmatrix}$$

The modeling of the shunt branch: The mathematical model of the UPFC shunt is given similarly by the following equations:

$$\begin{aligned} \frac{di_{pa}}{dt} &= -\frac{r_p}{L_p} \cdot i_{pa} + \frac{1}{L_p} \cdot (v_{pa} - v_{ca} - v_{ra}) \\ \frac{di_{pb}}{dt} &= -\frac{r_p}{L_p} \cdot i_{pb} + \frac{1}{L_p} \cdot (v_{pb} - v_{cb} - v_{rb}) \\ \frac{di_{pc}}{dt} &= -\frac{r_p}{L_p} \cdot i_{pc} + \frac{1}{L_p} \cdot (v_{pc} - v_{cc} - v_{rc}) \end{aligned} \quad (4)$$

With a transformation Park dq researchers have the system of Eq. (5):

$$\begin{aligned} \frac{di_{pd}}{dt} &= \omega \cdot i_{pq} - \frac{r_p}{L_p} \cdot i_{pd} + \frac{1}{L_p} (v_{pd} - v_{cd} - v_{rd}) \\ \frac{di_{pq}}{dt} &= -\omega \cdot i_{pd} - \frac{r_p}{L_p} \cdot i_{pq} + \frac{1}{L_p} (v_{pq} - v_{cq} - v_{rq}) \end{aligned} \quad (5)$$

The matrix form is given as follows:

$$\frac{d}{dt} \begin{bmatrix} i_{pd} \\ i_{pq} \end{bmatrix} = \begin{bmatrix} -r_p/l_p & -\omega \\ -\omega & -r_p/l_p \end{bmatrix} \begin{bmatrix} i_{pd} \\ i_{pq} \end{bmatrix} + \frac{1}{l} \begin{bmatrix} v_{sd} - v_{cd} - v_{rd} \\ v_{sq} - v_{cq} - v_{rq} \end{bmatrix}$$

The modeling of the UPFC continues branch: By passing on the principle of balance of power and neglecting the losses of the converters. The Dc voltage V_{dc} by the following equation:

$$\frac{dV_{dc}}{dt} = \frac{1}{C V_c} (p_e - p_{ep}) \quad (6)$$

Hence

$$p_e = v_{ca} i_{sa} + v_{cb} i_{sb} + v_{cc} i_{sc}$$

$$p_{ep} = v_{pa} i_{pa} + v_{pb} i_{pb} + v_{pc} i_{pc}$$

where,

p_e = Active power absorbed of the AC system

p_{ep} = Active power injected by the shunt inverter AC system

Applying the Park transformation on Eq. (6) researchers obtains:

$$\frac{dv_{dc}}{dt} = \frac{3}{2 C v_{dc}} (v_{pd} i_{pd} + v_{pq} i_{pq} - v_{cd} i_d - v_{cq} i_q) \quad (7)$$

The UPFC series and shunt UPFC's are identical in every respect. The commands used to set the inverter are the same for the shunt inverter.

CONTROLLER DESIGN

The objective of using the UPFC Fig. 1 is to provide independent control of active P and reactive Q power flow in the system for fixed values of V_s and V_r . This can be achieved by properly controlling the series injected voltage of the UPFC. The voltage, current and power flow are related through the following equations:

$$i_d^* = \frac{2}{3} \left(\frac{P^* \cdot V_{sd} - Q^* \cdot V_{sq}}{\Delta} \right) \quad (8)$$

$$i_q^* = \frac{2}{3} \left(\frac{P^* \cdot V_{sq} + Q^* \cdot V_{sd}}{\Delta} \right) \quad (9)$$

Here

$$\Delta = V_{sd}^2 + V_{sq}^2 \quad (10)$$

Once the desired active P^* and reactive Q^* power reference are known, (8) can be used to determine the corresponding i_d^* and i_q^* axes current references for the series convert. Similarly (8) can also be used to calculate the reference currents of the shunt converter but the variables P^* , Q^* , V_{sd} and V_{sq} are to be replaced by their respective sending end variables whenever appropriate.

It may be mentioned here that the Dc link voltage of the UPFC is to be kept at a constant value in the midst of disturbances. This can be achieved by generating an error signal between the desired Dc link voltage and the actual value. The error signal can be sent through another PI controller to obtain a command signal, which is subsequently added to the receiving-end power reference to drive the sending end power reference.

Decoupling PI control: According to the system of Eq. (3) or (5), one can have the system contains a coupling between the reactive and active current. The interaction between current loops caused by the coupling term (ω) Fig. 3. This explains the deviation of reactive power with respect to the reference. To reduce the interaction between the active and reactive power, a decoupling of the two current loops is needed.

The function of decoupling is to remove the product ωL and I_q controller along the axis d and adding the product term $\omega L I_d$ and the controller along the axis q. The design of the control system must begin with the selection of variables to adjust and then that of the control variables and their association with variables set. There is various adjustment techniques well suited to the PI controller. There are two well-

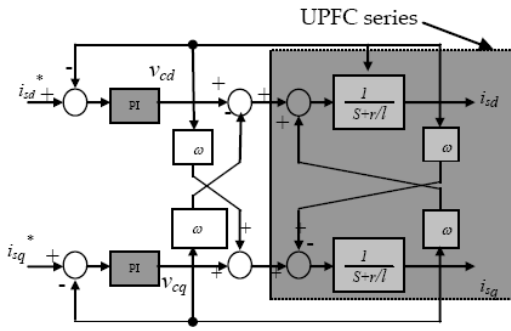


Fig. 3: Block diagram of the UPFC control (series)

Table 1: The parameters of the PI controller

$K_i = 20.000$	$K_p = 0.450$
$\omega_0 = 314.159$	$\zeta = 0.200$

known empirical approaches proposed by Ziegler and Tit for determining the optimal parameters of the PI controller (Ziegler and Nichols, 1942). The method Ziegler-Nichols, used in the present study is based on a trial conducted in closed loop with a simple analog proportional controller. The gain K_p of the regulator is gradually increased until the stability limit, which is characterized by a steady oscillation and measured by choice of the Table 1.

Based on the results obtained, the parameters of the PI controller given by Table 1.

SIMULATION RESULTS WITH PI-D UPFC

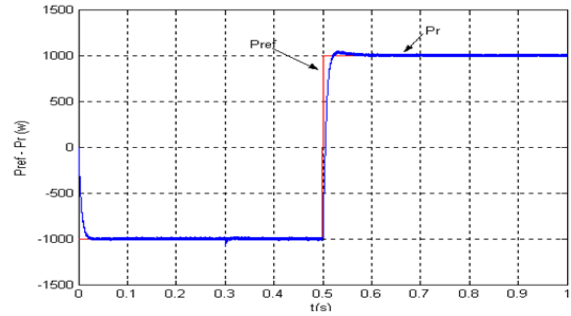
Figure 4 illustrates the behavior of active and reactive power, where we see that the control system has a fast dynamic response to the forces reach their steady states after a change in the reference values. We also note the presence of the interaction between the two components (d and q).

These influences are caused by the PWM inverter is unable to produce continuous signals needed by the decoupling, thus increasing the error in the PI-D controllers.

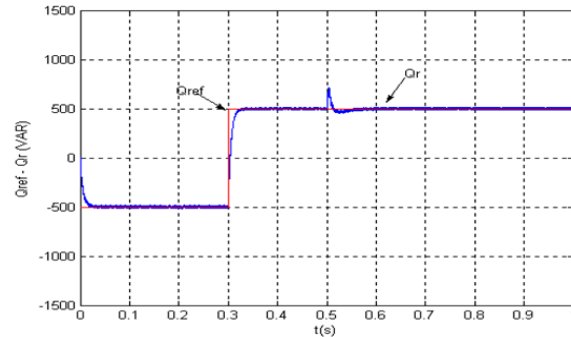
To test robustness, researchers tested the robustness for a variation of the reactance X_L 30% and I had variation on the output power following. Following these changes, the active and reactive power Fig. 5 undergo large deviations more or loss with an overflow at times of great change instructions (Pref, Qref), which means the performance degradation of the PI controller, interpreted by the loss of system stability.

Researchers simulated this time by introducing perturbation Fig. 6 duration of 25 ms and amplitude 1.5 to test again its robustness and system stability.

The response of active and reactive power at 30% of X_L could be detected; the error message given by MATLAB command indicated the saturation of the order at infinity in the spikes of the reference signals. One can check the response of the servo not only in continuation but also by adding a disturbance.

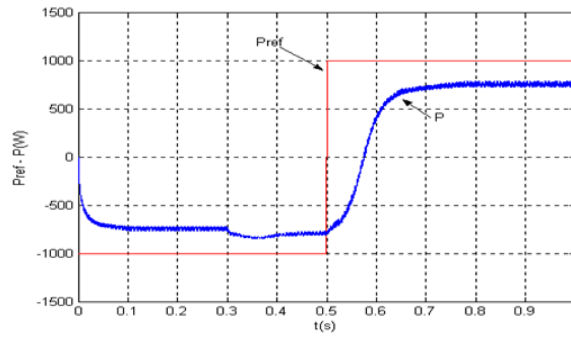


(a)

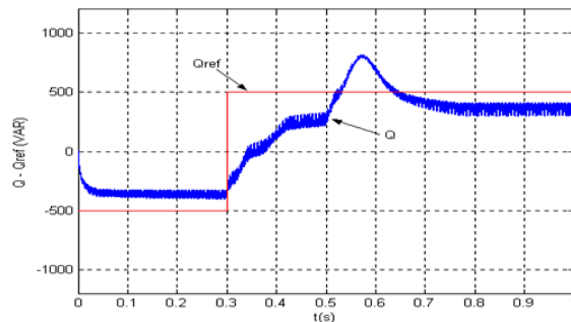


(b)

Fig. 4: Answers of powers with a PI-D

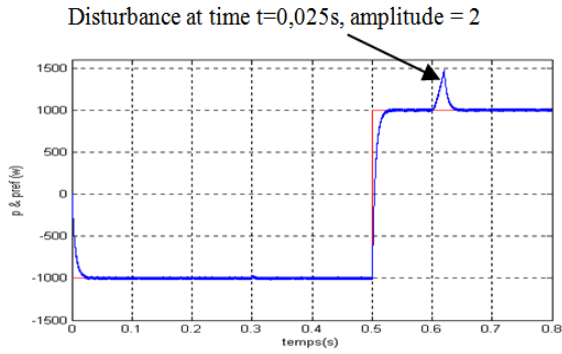


(a)

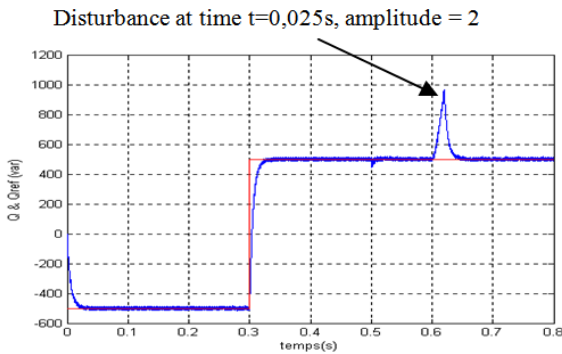


(b)

Fig. 5: Answers powers to change the reactance of 30%



(a)



(b)

Fig. 6: UPFC system perturbed to test stability

ADAPTIVE NEURAL CONTROL

The interest in adaptive control (Hingorani and Gyugyi, 2000) appears mainly at the level of parametric perturbations, we act on the characteristics of the process to be controlled and disturbances affect the variables control.

This study presents the method of adjustment proposed for The UPFC, by favoring the classical approach based on neural networks. Neural networks have shown great progress in identification of nonlinear systems. There are certain characteristics in ANN (Nguyen and Widrow, 1990) which assist them in identifying complex nonlinear systems.

Neural Network is made up of many nonlinear elements and this gives them an advantage over linear techniques in modeling nonlinear systems. Neural Network is trained (Chau, 2007) by adaptive learning, the network 'learns' how to do tasks, perform functions based on the data given for training. The knowledge learned during training is stored in the synaptic weights. The standard Neural Network structures (feed forward and recurrent) are both used to model the UPFC system.

The main task of this study is to design a neural network controller which keeps the UPFC system stabilized. Elman's network (Xiang *et al.*, 2002) said hidden layer network is a recurrent network, thus better suited for modeling dynamic systems.

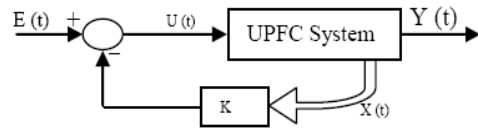


Fig. 7: Block diagram of a feedback control state of the UPFC

His choice in the neural control by state space is justified by the fact in particular the network can be interpreted as a state space model nonlinear. Learning by back propagation algorithm standard is the law used for identification of the UPFC.

State Space adaptive Neural control (SSNN): The integration of these two approaches (Denai and Allaoui, 2002) neural and adaptive control in a single hybrid structure, that each benefits from the other, but to change the dynamic behavior of the UPFC system was added against a reaction calculated from the state vector (state space) Fig. 7.

The state feedback control is to consider the process model in the form of an equation of state:

$$X^*(t) = Ax(t) + Bu(t) \quad (11)$$

And observation equation:

$$Y(t) = Cx(t) + Du(t) \quad (12)$$

where,

$u(t)$ = The control vector

$x(t)$ = The state vector

$y(t)$ = The output vector of dimension for a discrete system to the sampling process parameters T_e at times of T_e sample k are formalized as follows:

$$X(t+1) = A_d x(t) + B_d u_d(t) \quad (13)$$

$$Y(t) = C_d x(t) + D_d u(t) \quad (14)$$

The transfer function $G(s) = Y(s) / U(s)$ of our process UPFC can be written as:

$$G(s) = \frac{1}{s + r/L} \quad (15)$$

We deduce the equations of state representation of the UPFC:

$$\begin{cases} \dot{x}^* = -\left(\frac{r}{L}\right)x + u \\ y = x \end{cases} \quad (16)$$

with,

$$U(t) = e(t) - kx(t)$$

Let:

$$X(t+1) = [A_d - KB_d]x(t) + B_d e(t) \quad (17)$$

$$Y(t) = C_d x(t) \quad (18)$$

The dynamics of the process corrected by state space is presented based on the characteristic equation of the matrix $[A_d - B_d K]$, where K is the matrix state space controlled process. The system is described in matrix form in the state space:

$$\begin{cases} \dot{x}^* = A.x + B.u \\ y = C.x + D.u \end{cases} \quad (19)$$

where,

$$A = \begin{bmatrix} \frac{-r}{L} & \omega \\ -\omega & \frac{-r}{L} \end{bmatrix} \quad B = \begin{bmatrix} \frac{-1}{L} & 0 \\ 0 & \frac{-1}{L} \end{bmatrix} \quad C = \begin{bmatrix} 1 & 0 \\ 0 & 1 \end{bmatrix} \quad D = \begin{bmatrix} 0 & 0 \\ 0 & 0 \end{bmatrix}$$

$$u = \begin{bmatrix} v_{cd} \\ v_{cq} \end{bmatrix} \quad y = \begin{bmatrix} i_{sd} \\ i_{sq} \end{bmatrix} \quad x = [i_{sd} \quad i_{sq}]^T$$

IDENTIFICATION BASED NETWORK ELMAN

Process identified (Zebirate *et al.*, 2004; Xie *et al.*, 2006) will be characterized by the model structure Fig. 8, of his order and parameter values. It is therefore, a corollary of the simulation process for which using a model and a set of coefficients to predict the response of the system. The Elman network (Xiang *et al.*, 2002) consists of three layers: an input layer, hidden layer and output layer. The layers of input and output interfere with the external environment, which is not the case for the intermediate layer called hidden layer i.e., the network input is the command $U(t)$ and its output is $Y(t)$.

The state vector $X(t)$ from the hidden layer is injected into the input layer. Researchers deduce the following equations:

$$X(t) = W_r X(t-1) + W_h U(t-1) \quad (20)$$

$$Y(t) = W_o X(t) \quad (21)$$

where, W_h ; W_r & W_o are the weight matrices. Equations are standard descriptions of the state space of dynamical systems. The order of the system depends on the number of states equals the number of hidden

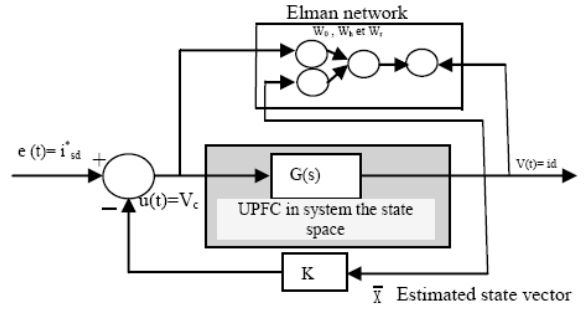


Fig. 8: Network Elman and state space

layers. When an input-output data is presented to the network at iteration k squared error at the output of the network is defined as:

$$E_t = \frac{1}{2} (y_d(t) - y(t))^2 \quad (22)$$

For all data $u(t)$, $y_d(t)$ de $t = 1, 2, \dots, N$, the sum of squared errors is:

$$E = \sum_{t=1}^N E_t \quad (23)$$

At each iteration, the weights are modified for W_0 we have:

$$\begin{aligned} \frac{\partial E_t}{\partial W_0} &= -(y_d(t) - y(t)) \frac{\partial y(t)}{\partial W_0} \\ &= -(y_d(t) - y(t)) x^T(t) \end{aligned} \quad (24)$$

For W_h et W_r :
where,

$$\begin{aligned} \frac{\partial E_t}{\partial W_h} &= -\frac{\partial E_t}{\partial y(t)} \cdot \frac{\partial y(t)}{\partial x(t)} \cdot \frac{\partial x(t)}{\partial W_h} \\ &= -(y_d(t) - y(t)) W_0^T \cdot u(t) \end{aligned} \quad (25)$$

$$\begin{aligned} \frac{\partial E_t}{\partial W_r^i} &= -\frac{\partial E_t}{\partial y(t)} \cdot \frac{\partial y(t)}{\partial x_i(t)} \cdot \frac{\partial x_i(t)}{\partial W_r^i} \\ &= -(y_d(t) - y(t)) W_0^i \frac{\partial x_i(t)}{\partial W_r^i} \end{aligned} \quad (26)$$

The latter we obtain:

$$\frac{\partial x_i}{\partial W_r^i} = X^T(t-1) + W_r^i \cdot \frac{\partial x(t-1)}{\partial W_r^i} \quad (27)$$

The variation of the weight matrix based on the learning gain is written as:

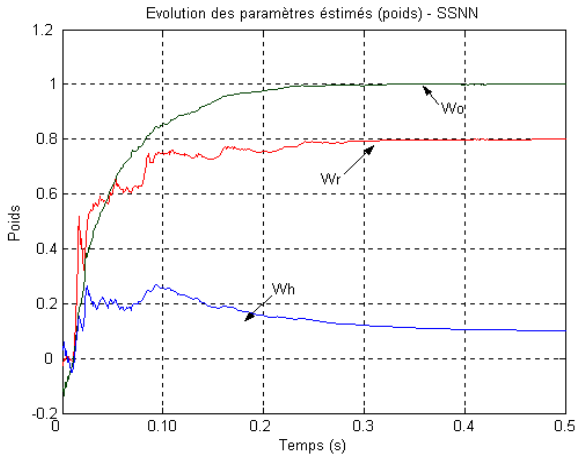


Fig. 9: Changing weight

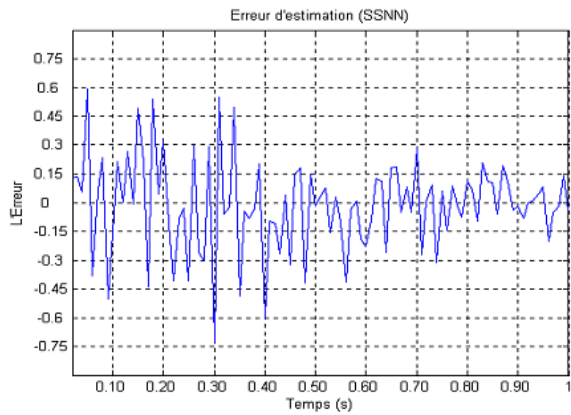


Fig. 10: Estimation error

$$\Delta W = -\eta \cdot \frac{\partial E_t}{\partial W} \quad (28)$$

Note that the performance of the identification is better when the input signal is sufficiently high in frequency to excite the different modes of process. The three weights W_o , W_r and W_h Which are respectively.

The matrices of the equation of state of the process system (UPFC) (CA and B) became stable after a rough time $T = 0.3s$ and several iterations Fig. 9. (For the Elman network neuron type is assumed through the vector is zero ($D = 0$)).

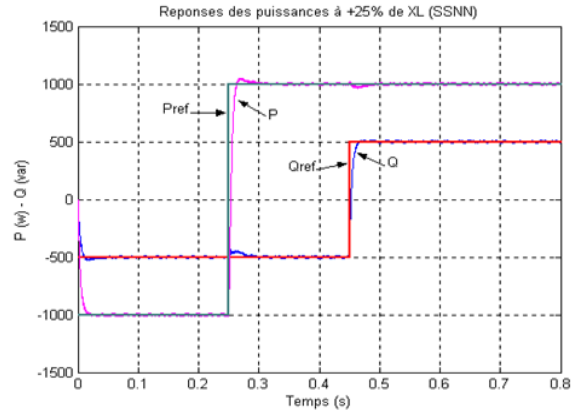
In online learning Elman network, the task of identifying and correcting same synthesis are one after the other. Or correction of the numerical values of the parameters is done repeatedly so the estimation error.

Figure 10 takes about almost a second ($t = 1s$) to converge to zero i, regulation in pursuit.

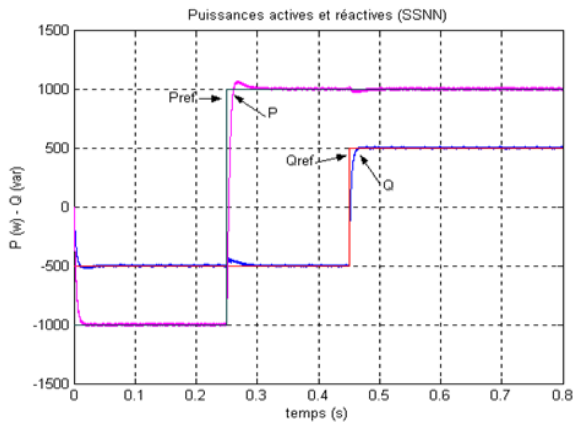
Robustness test: To check the robustness to the controller, two tests were performed. For each test we varied the parameters (Yu *et al.*, 1996) which are listed in Table 2 of the transmission line but the controller remains unchanged.

Table 2: The parameters of the laboratory UPFC model

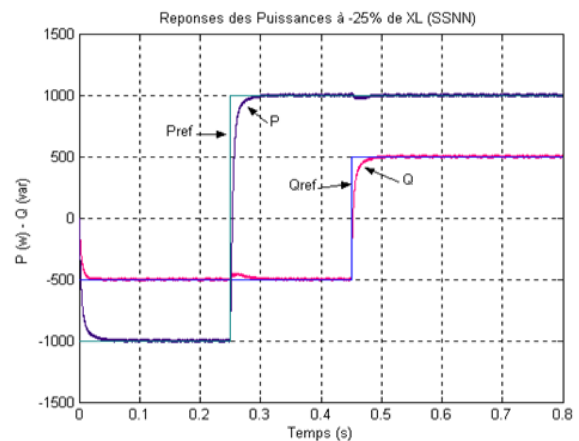
V_t	220 V	R_p	0.4 Ω
V_s	220 V	R	0.8 Ω
C	2 mF	L_p	10 H
V^*dc	280 V	L	10 H



(a)



(b)



(c)

Fig. 11: Neural adaptive control (SSNN) powers P, Q and at ($\pm 25\%$ XL)

It can be seen that the variation of the reactance ($\pm 25\%$) has almost no influence on the output characteristics of the UPFC system Fig. 11. To compare the responses of active and reactive power of UPFC system, Researchers gave the three cases Fig. 11 Where (a) and (c) are the responses to changes ($\pm 25\%$) and (b) is the response of the system without any change in reactance.

CONCLUSION

The identification process will be characterized by the model structure, its order and parameter values. It is therefore a corollary of the simulation process which uses a model and a set of coefficients to predict the response of the system. The use of more advanced low-identification neural network can be dependable in the calculation algorithm of the order.

Note that the performance of the identification of system parameters a neuron network said Elman network with three layers. As we have already seen. Note that the performance of the identification is better when the input signal is sufficiently high in frequency to excite the different modes of process. Neural adaptive control by state feedback (SSNN: State Space Neural Network) is a hybrid control based on the representation of system status UPFC was tested. The performance of the latter are slightly degraded, this is may be due to the delay caused by the algorithm, it cannot be reduced at will, or it may due to the choice of the gain K of the closed loop.

Finally, the identification process based on learning of Elman neural network, provides the dynamic behavior of the process and to estimate the system output as its state vector based on the information that are control signal and the measured output.

The simulation results of the proposed controller are compared with a conventional PI controller and its performance is evaluated. In this study, the sending and receiving end bus voltages were maintained constant and the dc link voltage, active and reactive powers of the transmission line were controlled. The obtained results from above case studies describe the power, accuracy, fast speed and any overshoot response of the proposed controller.

REFERENCES

- Chau, K.W., 2007. Reliability and performance-based design by artificial neural network. *Adv. Eng. Software*, 38: 145-149.
- Chau, K.W., C.L. Wu and Y.S. Li, 2005. Comparison of several flood forecasting models in Yangtze River. *J. Hydrol. Eng.*, 10: 485-491.
- Denai, M.A. and T. Allaoui, 2002. Adaptive fuzzy decoupling of UPFC-power flow compensation. 37th UPEC2002, September 9-11, Straffordshires University, UK.
- Edris, A., L. Gyugi, T. Riedman and D. Torgerson, 1996. The Unified Power Flow Controller (UPFC) for multiple power transmission compensation. *ETG- FACHBERICHT*, 60: 61-78.
- Gyugyi, L., 1992. Unified power flow control concept for flexible AC transmission systems. *IEE Proc.*, 139: 323-331.
- Henriques, J. and A. Dourado, 1999. A hybrid neural-decoupling pole placement controller and its application. *Proceeding of 5th European Control Conference (ECC99)*. Karlsruhe, Germany.
- Hingorani, N.G. and L. Gyugyi, 2000. *Understanding FACTS: Concepts and Technology of Flexible AC Transmission Systems*. IEEE Press, NY.
- Lin, J.Y., C.T. Cheng and K.W. Chau, 2006. Using support vector machines for long-term discharge prediction. *Hydrol. Sci. J.*, 51: 599-612.
- Ma, T.T., 2003. Enhancement of power transmission systems by using multiple UPFCs on evolutionary programming. *Proceeding of IEEE Bologna Power Tech Conference*, 4: 23-26.
- Narain, G.H. and G. Laszlo, 1999. *Understanding FACTS: Concepts and Technology of Flexible AC Transmission Systems*. Wiley-IEEE Press Marketing, pp: 297-352; 407-424.
- Nguyen, D. and B. Widrow, 1990. Neural networks for self-learning control systems. *IEEE Control Syst. Mag.*, 10(3): 18-23.
- Papic, I., P. Zunko, D. Povh and M. Weinhold, 1997. Basic control of unified power flow controller. *IEEE T. Power Syst.*, 12(4): 1734-1739.
- Schoder, K., A. Hasanovic and A. Feliachi, 2000. Fuzzy damping control for the Unified Power Flow Controller (UPFC). *Proceeding of North America Power Symposium*. Waterloo, Canada, 2: 521-527.
- Sen, K.K. and A.J.F. Keri, 2003. Comparison of field results and digital simulation results of voltage-sourced converter-based facts controllers. *IEEE T. Power Deliver.*, 18: 300-306.
- Tuttas, C., 1999. Power Flow control of series compensated transmission lines with an UPFC. *Proceedings of European Power Electronics Conference (EPE'99)*. Lausanne, pp: 1-10.
- Xiang, L., C. Guanrong, C. Zengqian and Z. Yuan, 2002. Chaotifying linear Elman networks. *IEEE T. Neural Networ.*, 13(5): 1193-1199.
- Xie, J.X., C.T. Cheng, K.W. Chau and Y.Z. Pei, 2006. A hybrid adaptive time-delay neural network model for multi-step-ahead prediction of sunspot activity. *Int. J. Environ. Poll.*, 28: 364-381.

- Yu, Q., S.D. Round, L.E. Norum and T.M. Undeland, 1996. Dynamic control of a unified power flow controller. Proceeding of 27th Annual IEEE Power Electronics Specialists Conference (PESC '96) Record. Baveno, 1: 508-514.
- Zebirate, S., A. Chaker and A. Feliachi, 2004. Neural network control of the unified power flow controller. Proceeding of IEEE Power Engineering Society General Meeting, 1: 536-541.
- Zhengyu, H., N. Yinxin, C.M. Shen, F.F. Wu, C. Shousun and Z. Baolin, 2000. Application of unified power flow controller in interconnected power systems-modeling, interface, control strategy and case study. IEEE T. Power Syst., 15: 817-824.
- Ziegler, J.G. and N.B. Nichols, 1942. Optimum settings for automatic controllers. Trans. ASME, 64: 759-768.